1-1-2010

Selection of integration time intervals for quartz OSL decay curves

Alastair C. Cunningham
Delft University of Technology, acunning@uow.edu.au

Jakob Wallinga
Delft University of Technology

Selection of integration time intervals for quartz OSL decay curves

Abstract

In quartz optically stimulated luminescence (OSL) dating protocols, an initial integral of the OSL decay curve is used in the calculation of equivalent dose, once a background integral has been subtracted. Because the OSL signal commonly contains a number of exponentially decaying components, the exact choice of time intervals used for the initial-signal and background integrals determines the composition of the net signal. Here we investigate which combination of time intervals will produce the net signal most dominated by the fast OSL component, while keeping an acceptable level of precision. Using a three-component model of OSL decay, we show that for a specified level of precision, the net signal most dominated by the fast component can be obtained when the background integral immediately follows the initial signal and is approximately 2.5 times its length. With this 'early-background' approach, the contribution of slow components to the net signal is virtually zero. We apply our methods to four samples from relatively young deposits. Compared to the widely used 'late-background' approach, in which the background integral is taken from the last few seconds of OSL, we find less thermal transfer, less recuperation and a higher proportion of aliquots yielding an equivalent dose in agreement with expectations. We find the use of an early background to be a simple and effective way of improving the accuracy of OSL dating, and suggest is should be used in standard protocols.

Keywords

CAS

Disciplines

Medicine and Health Sciences | Social and Behavioral Sciences

Publication Details

Cunningham, A. C. & Wallinga, J. (2010). Selection of integration time intervals for quartz OSL decay curves. Quaternary Geochronology, 5 (6), 657-666.

Selection of integration time-intervals for quartz OSL decay curves

Alastair C. Cunningham[1,*], Jakob Wallinga[1]

1 Netherlands Centre for Luminescence dating, Delft University of Technology, Faculty of Applied Sciences, Mekelweg 15, 2629 JB Delft, the Netherlands

Abstract

In quartz optically stimulated luminescence (OSL) dating protocols, an initial integral of the OSL decay curve is used in the calculation of equivalent dose, once a background integral has been subtracted. Because the OSL signal commonly contains a number of exponentially decaying components, the exact choice of time intervals used for the initial-signal and background integrals determines the composition of the net signal. Here we investigate which combination of time-intervals will produce the net signal most dominated by the fast OSL component, while keeping an acceptable level of precision. Using a three-component model of OSL decay, we show that for a specified level of precision, the net signal most dominated by the fast component can be obtained when the background integral immediately follows the initial signal and is approximately 2.5 times its length. With this 'early background' approach, the contribution of slow components to the net signal is virtually zero. We apply our methods to four samples from relatively young deposits. Compared to the widely used 'late background' approach, in which the background integral is taken from the last few seconds of OSL, we find less thermal transfer, less recuperation and a higher proportion of aliquots yielding an equivalent dose in agreement with expectations. We find the use of an early background to be a simple and effective way of improving the accuracy of OSL dating, and suggest is should be used in standard protocols.

Keywords: OSL; luminescence dating; quartz; partial bleaching; integration time-intervals; early background; channels

1. Introduction

In the dating of quartz grains using Optically Stimulated Luminescence (OSL), the OSL signal is commonly measured by stimulating the sample with blue light at a constant intensity for several tens of seconds, while holding the sample at approximately 125ºC. Under such Continuous Wave (CW) stimulation, the OSL signal measured in the UV region decays over a number of seconds. Some portion of the decay curve is used for the calculation of equivalent dose (D_e), once corrected for sensitivity change, and calibrated against the OSL response to one or more known doses (e.g. the Single Aliquot Regenerative dose (SAR) protocol of Murray and Wintle, 2000). However, the quartz OSL decay curve consists of a number of first-order exponential components, corresponding to different trap types in the quartz crystal (Smith and Rhodes, 1994; Bailey et al., 1997; Jain et al., 2003). The 'fast' component has been identified as the most suitable for dating, as it is stable on geological timescales, rapidly bleached by sunlight, and less susceptible to thermal transfer of charge (Wintle and Murray, 2006). Moreover, the SAR protocol has been designed and tested for samples dominated by the fast component. It is therefore desirable to use measurement procedures that maximise the influence of the fast component on D_e.

In typical OSL dating protocols, the integrated photon count from the initial part of the decay curve is used for D_e determination, after subtracting the integrated photon count from the last few seconds of decay. In a multi-component system however, the choice of time-intervals used for the 'initial signal' and 'background' inevitably influence the proportion of the net signal that comes from each component. While it is not possible to isolate the fast component through background subtraction, it is possible to maximise its contribution. The optimum choice of time-intervals depends on the relative magnitude of each component and their photo-ionisation cross-sections, the intensity and wavelength of stimulation light, the signal-to-noise ratio, and the desired measurement precision. The optimum time-intervals therefore vary between instruments, samples and even aliquots.

The aim of this paper is to identify the most appropriate time-intervals for practical use in quartz CW-OSL dating, assuming that the fast component is both present and desired, and 470 nm stimulation light is used. We focus primarily on the dating of young samples, for two reasons: 1) young samples are more susceptible to effects of thermal transfer and partial bleaching, resulting in different D_e for different components; and 2) for young samples, the application of methods to isolate the fast component is challenging because of poor signal-to-noise ratios.

2. Samples and equipment

In this study we make use of four samples from the Netherlands. The samples are all relatively young, and were deposited under less than ideal bleaching conditions. Since different components bleach at different rates, we expect the calculated ages to depend on the choice of time-intervals used. Two of the samples also benefit from good age control.

- Sample NCL-3505030 is from a recent floodplain deposit of the River Waal. Historical maps of the area indicate that the section of floodplain from which the sample was taken was formed between 1723 and 1810 AD (Middelkoop, 1997; Bakker et al., 2007).
- Sample NCL-1109004 is from a storm-surge sediment (consisting mostly of sand) collected from the coastal dunes of North Holland. A large series of OSL dates from the site indicate that the sample was deposited in the late 18^{th} century, and a comparison with documentary sources suggests a likely date of deposition of AD 1775 or 1776 (Cunningham et al., 2009).
- Sample NCL-1107136 is from a very young embanked floodplain of the River Waal (Hobo et. al, 2010). Stratigraphically consistent OSL ages for the site have been provided by Wallinga et al. (2010), from which we can be confident that the deposition age is < 55 a.
- Sample NCL-9908154 comes from sandy sediments sampled just below a Medieval rampart structure near Nijkerk (Doesburg et al., 2010). Depositional environment, bleaching conditions and age of the sample are not known.

Prior to measurement, samples were sieved and treated with HCl, H_2O_2 and HF to isolate the quartz fraction. OSL measurements were carried out on Risø TL-DA-15 readers (Bøtter-Jensen et al., 2000). Stimulation was with 470 nm blue diodes with a power at the sample position of ~35 mW cm^{-2}. One reader had a higher stimulation power, for which corrections were made in analysis. Irradiation was with $^{90}Sr/^{90}Y$ beta sources providing dose rates between 0.028 and 0.14 Gy s^{-1} to quartz grains at the sample position. The IR diodes emitted at a wavelength of 875 nm and power of ~116 mW cm^{-2}. A 7.5mm Hoya U340 detection filter was used.

OSL measurements are based on the SAR protocol of Murray and Wintle (2000; 2003), details of which are given in Table 1. OSL was measured using a channel step-size of 0.05 s unless stated (this step-size is also used in the calculations of Section 3). Preheat conditions were selected on the basis of a thermal transfer test (Section 4.3). The grainsize used was 180 to 212 µm (NCL-1109004 and NCL-9908154), 212 to 250 µm (NCL-3505030), and 180 to 250 µm

(NCL 1107136), with each aliquot containing about 200 to 300 grains. Three samples were expected to indicate a dose of less the 0.5 Gy, for which it is not necessary to ascertain the saturation point of the dose-response curve. For this reason, and to reduce measurement time, the regenerative dose curve for these three samples was constructed with a single (small) given-dose and forced through the origin (see chapter 6 of Ballarini (2006)) for a discussion on this point). For sample NCL-3505030 we included a 175ºC IR bleach for 40 s prior to each OSL step, to reduce the effect of any remaining feldspar grains or inclusions (Wallinga et al., 2002). This IR beaching step is likely to deplete the fast OSL component by a very small amount (~0.5 %) in both the natural and regenerative signal (derived from Jain et al. (2005)). The OSL following zero dose was measured, followed by a repeat of the first given dose. For D_e calculations, aliquots were accepted only if the recuperated dose was less than 0.05 Gy, and the recycling ratio was within 10% of unity. For very young sample NCL-1107136, permissible recuperation values included those consistent with zero within one standard error. To estimate the environmental dose rate to our samples we used a high-resolution gamma ray spectrometer, after preparing our samples using the procedure described in Wallinga et al. (2010).

Place table 1 here

3. Methods

3.1 Early background subtraction

Standard practice for selection of integration time-intervals follows Banerjee et al. (2000), with an initial integral of the decay curve (e.g. 0 - 0.30 s) usually taken as indicative of the fast component signal, once a late background (e.g. 36 - 40 s) has been subtracted (and corrected to the length of the initial signal). Using the last few seconds of the decay as background adequately removes photomultiplier dark noise and stimulation light leakage from the signal, and also subtracts the majority of the slow component. The length of the initial signal is usually kept short, since the shorter it is, the larger the proportion of fast component in the net signal.

However, since the fast component is usually the most rapidly decaying, it follows that to maximize the proportion of fast component in the net signal, the time-interval used for the background subtraction should immediately follow that of the initial signal. Such a procedure has been hinted at before (Aitken and Xie, 1992; Singhvi and Lang, 1998; Ballarini et al., 2007), but has not yet become standard practice, perhaps because of the detrimental effect on measurement

precision. No comprehensive analysis of time-interval choice has yet been published, so we explore this topic in the following sections.

3.2 Selection of time-intervals

The choice of channels used for defining the 'initial signal' and 'background' integrals determine the proportion of each component in the net signal, and the relative error due to counting statistics. Moreover, for any choice of time-intervals the proportion of each component in the net signal will vary between aliquots due to variations in the intensity and decay rate of each OSL component between grains. To understand how the composition of the net OSL signal is influenced by the choice of integration time intervals, we discuss first a simulated decay curve. The simulated curve used here consists of three exponentially decaying components of the form $n_{0i}\alpha_i exp(-\alpha_i t)$, where t is time (s), n_{0i} is the initial population of component i, and α_i is the decay rate of component i. The decay rate of each component is governed by its photoionisation cross-section at the stimulation wavelength, and the intensity of stimulation light. The decay rates used here ($\alpha_1 = 2.2\ s^{-1}$, $\alpha_2 = 0.44\ s^{-1}$, $\alpha_3 = 0.02\ s^{-1}$) were determined during a previous curve-fitting exercise (Cunningham and Wallinga, 2009), and are broadly representative of the fast, medium and slow2 components of Jain et al. (2003) under (470 nm wavelength) stimulation light intensity of ~35 mW cm^{-2}. The populations n_{0i} in this example are 100, 100 and 1000; i.e. the same trap populations for the fast and medium components, with a much larger slow component. The simulated decay curve was produced with 0.05 s time-steps, and for clarity no noise was included. Using this simulated decay curve, the contribution of each component to the net OSL signal can be calculated for every time-interval combination used for signal and background collection. The error due to counting statistics can also be determined, and is given henceforth as the Relative Standard Error (RSE) term of Li (2007).

The results of this exercise can be seen in Fig. 2. In Fig. (1a), the proportion of fast component in the simulated net OSL signal is shown as a function of the time-interval used for the initial signal and the time-interval used for the background subtraction (which is taken immediately following the initial signal). The horizontal plane indicates the equivalent value calculated using the 'Late background' time-intervals (0 – 0.30 s for the initial signal, 36 - 40 s for the background). Figs (1b-c) show the same for the medium and slow components. It is clear that the slow component is almost wholly removed with any combination of early background time-intervals. It is also evident from these plots that the maximisation of the fast component and minimisation of the medium component is best achieved by using a short time interval for the

initial signal, and a short time interval for the background. However, the use of short time intervals, especially for the background, leads to a reduction in the precision with which the net signal is known (Fig. 1d). It is therefore necessary to introduce some criteria for an acceptable level of precision. The best combination of time-intervals is the one which gives the net signal with the largest percentage of fast component, while keeping the RSE below this threshold. Some criteria are therefore needed to select the best channel combination. As an example, we have plotted an RSE threshold of 5% as a horizontal plane on Fig. 1d. The combination of time-intervals which gives the largest proportion of the net signal from the fast component while satisfying the RSE criteria is indicated by the black square on Fig. 1a.

Place figure 1 here

4. Results

4.1 Validation of the 3-component model

Example (regenerative) decay curves have been fitted with three (unconstrained) components, and are plotted in Fig. 2. The parameters vary slightly between each plot, as expected. All samples have a fast and slow component. While sample NCL-9908154 has little or no medium component, a three component model can still be applied (which mean the n_{02} parameter will equal zero, or be very small).

Place figure 2 here

4.2 Calculations for real data

In order to perform time-interval calculations for real OSL decay curves, it is necessary to first estimate the magnitude of the various components. Here we have applied a simple curve-fitting routine to decay curves following a regenerative dose given to 24 aliquots of each sample. By assuming a maximum of three components are present, and their photo-ionisation cross-sections are predetermined, it is computationally simple to gain an approximation of the magnitude of each component using a non-negative least squares method. As no variation in decay rate α is permitted, the outcome does not give a rigorous fit, but provides a good approximation of the magnitude of each component. With an estimate of the decay-curve composition, the calculation of the optimal integration time-intervals can be done according to the method outlined in Section

3.2, which now depends solely on the desired level of precision. The influence of desired precision on time-interval selection is shown in Fig. 3, for two aliquots of sample NCL-3505030. For aliquot (a), a reduction in the precision threshold (an increase in RSE) allows the proportion of fast component in the net signal to be increased, which is achieved by decreasing the length of the integration time-intervals for both the initial-signal and (subsequent) background intervals. However, it is apparent that the improvement in the percentage of fast component gained through a reduction in precision suffers from diminishing returns, with little benefit obtained by increasing the RSE beyond 2.5%. Fig. 3b shows the same information for an aliquot with a less dominant fast component. In this case, a significant improvement in the proportion of fast component can be achieved by accepting less precision.

It is important to note that for both aliquots shown in Fig. 3 the implied range of suitable integration lengths is similar. Furthermore, as the RSE threshold is changed, the relationship between signal length and background length is similar for all four samples. This can be seen more clearly in Fig. 4, which plots the optimum background-length to signal-length ratio for 24 aliquots of each sample, as a function of RSE threshold. Each strand represents one aliquot, which has had its component magnitudes n_{0i} estimated using the constrained fitting described above. For each RSE threshold on the regenerative signal, the channel combination resulting in the net signal most dominated by the fast component was identified, and the ratio plotted. Sample NCL-3505030 (Fig. 4a) has relatively weak signals, with a dominant slow component (Fig. 2a). For less stringent (for this sample) RSE thresholds of 10-15 % (which leads to shorter integration lengths), the ratio for all aliquots lies between two and four. As the RSE threshold is made more stringent (leading to longer integration lengths), aliquots with a more dominant fast component tend to keep this ratio. For aliquots with less fast component, the RSE threshold can only be achieved by using a very long background interval, leading to a high ratio. For many aliquots in this example, it is not possible to obtain a stringent RSE. For sample NCL-1109004 we can see a similar pattern, with the ratio staying mostly between 2 and 3. Samples NCL-1107136 and NCL-9908154 are characterised by a much more dominant fast component (Fig. 2c and 2d), and for more stringent RSEs have a ratio close to 2.5. Because the regenerative signals from these samples are strong, relaxation of the RSE threshold leads to very short integration lengths, causing sharp jumps in the ratio.

While the level of precision ultimately chosen may be arbitrary, it is important to note that the ratio of background length to signal length required to maximise the fast component remains between 2 and 3, and this ratio holds across a greater range of RSE thresholds for aliquots with a more dominant fast component. In practice, the length of the time-intervals may

be governed by the signal-to-noise ratio, but the ratio of background length to signal length should remain between 2 and 3. For the samples shown here, we kept this ratio at 2.5, but changed the integration lengths according to signal strength. For samples NCL-3505030 and NCL-1109004 (estimated age between 200 and 300 a) we used signal and background intervals of [0 – 0.40; 0.40 – 1.40 s] (Fig. 5a and b). Sample NCL-1107136 has a very weak natural signal, so to ensure enough signal was collected for acceptable precision, the integration intervals were lengthened to [0 – 0.60; 0.60 – 2.10 s]. Sample NCL-9908154 is far more sensitive to OSL, and we were able to reduce the length of the integration intervals to [0 – 0.20; 0.20 – 0.70 s] while maintaining reasonable precision.

Place figure 3 here

Place figure 4 here

4.3 Thermal transfer

Our OSL measurements are preceded by a preheat, the purpose of which is to empty thermally unstable OSL traps which would otherwise contribute to the signal. However, preheating can lead to thermal transfer of charge from light-insensitive traps (which may contain large accumulated doses), to the traps responsible for OSL (Wintle and Murray, 2006). This is a particular problem for young samples given their comparatively small D_e. When this occurs following the regenerative doses, it is detectable in the OSL following a zero dose (recuperation). Based on curve fitting the OSL signals, Jain et al. (2003) and Tsukamoto et al. (2003) found the fast component to show far less recuperation than the medium or slow components.

If the D_e calculated using the early background is indeed a better reflection of the fast component D_e, we would expect to see less thermal transfer and recuperation than with the late background. To test for thermal transfer, we first bleached eight aliquots of each sample with 470 nm LEDs at room temperature for 40 s, which was repeated after a 1000 s pause. This treatment aims to empty trapped charge giving rise to the fast (and medium) component, whilst leaving a large part of the less light-sensitive trapped charge in place. A low (140ºC) preheat was then given, followed by OSL at 125ºC. Successive preheats to higher temperatures (160ºC, 180ºC … 220ºC) were then applied, each followed by an OSL measurement. Finally the OSL signal was reset by a high temperature bleach, after which the OSL response to a single dose point was measured to allow translation of the thermal transfer OSL signals to an approximate D_e. The cumulative D_e indicates the amount of thermal transfer at each preheat temperature, albeit with a

slight temperature shift caused by the earlier preheats. This procedure is explained fully in Wallinga et al. (2009), and differs slightly from the approach of Jain et al. (2004) and Truelsen and Wallinga (2003) in that no test dose is given. The results clearly show that less thermal transfer is measured if the early background is used (Fig. 5c and d). Measurements of recuperation also yield lower values for the early background than for the late background (Table 2).

Place table 2 here

Place figure 5 here

4.4 Equivalent dose

The use of the early background has a significant effect on the D_e distribution for three of the samples shown here. For fluvial sample NCL-3505030 (Fig. 6a-c), the reduction in the measured recuperation values when the early background is used lead to more aliquots passing the acceptance criteria. There is a reduction in D_e compared with the late background for most aliquots, which could be due to the reduction in thermal transfer and/or smaller contributions from less light-sensitive components. More aliquots, and a higher proportion of aliquots, give results in agreement with the expected D_e. For storm-surge deposited sample NCL-1109004, the impact of partial bleaching and thermal transfer are less obvious, but the early background still has a beneficial effect on D_e. While less aliquots pass acceptance criteria than with the late background, those which remain show a tighter distribution, and are largely in agreement with the expected D_e (Fig. 6d-f).

Probability density functions (PDFs) of D_e for samples NCL-1107136 and NCL-9908154 can be seen in Fig. 7, along with example decay curves. The PDF plots appear to show early background datasets which are more in line with the expected results than the late-background counterparts. For sample NCL-9908154 this is a little surprising – decay curves from this sample show virtually no medium or slow components (e.g. Fig. 2d), so we would not expect the choice of integration intervals to affect D_e. The difference may be due to random effects, e.g. which aliquots happen to pass acceptance criteria; it may be due to the larger errors in the EBG dataset for this sample; or perhaps because the error term of Li (2007) employed here is more appropriate for use with the early background (as it assumes there is no slow component in the net signal).

Place figure 6 here

Place figure 7 here

5. Discussion

5.1 Implications of early background subtraction for young samples

For the young samples studied here, it is clear that the use of the early background time-intervals has a beneficial effect on the D_e distribution, by increasing the number and proportion of accepted aliquots which have D_e consistent with a single population, and also with the expected D_e. This is achieved through two effects:

1. *The almost complete removal of the slow component from the net signal*. The proportion of the net signal belonging to the slow component is an order of magnitude less with the early background compared to the late background (Fig.1c). This results in a significant and consistent reduction in the measured amounts of thermal transfer and recuperation, and is likely to lessen the severity of partial bleaching in the D_e distribution. Differences in the precise choice of early background intervals have a minor effect on the D_e distribution, which implies that the removal of the slow component is the most important effect (since the slow component is removed by any combination of early background time-intervals). Ballarini et al. (2007) also came to this conclusion when testing integration intervals for single-grain measurements, although the 525 nm stimulation wavelength they used would have lead to a larger difference in the photoionisation cross-sections of the fast and medium components (Singarayer and Bailey, 2004).
2. *Improved auto-weighting of aliquots according to the dominance of the fast component.* When the early background is used, aliquots with little or no fast component will tend to give imprecise D_e. The resulting D_e distribution is then naturally weighted towards aliquots with a strong fast component, as they retain a relatively precise D_e. Any age model then applied to the D_e dataset, provided it takes account of the errors on each aliquot (e.g. central and minimum age models of Galbraith et al. (1999)), will be preferentially influenced by the desirable, fast-component dominated aliquots. This may result, for instance, in a reduction in the

number of apparent age populations and an increase in precision on the age-model derived D_e.

Use of an early background may also reduce the feldspar component of the 'quartz' signal. Although standard laboratory preparation for quartz includes chemical treatment to remove feldspars, there can often be a remnant signal from, for instance, feldspar inclusions within quartz grains (Huntley et al., 1993). Since feldspar OSL decay is slower than quartz under 470 nm stimulation (e.g. Wallinga et al., 2002), the use of an early background will remove more of the feldspar signal than with a late background.

5.2 Sensitivity in the choice of early background time-intervals

Complete isolation of the fast component is not possible with any combination of integration time-intervals, if there are other components present in the signal. The percentage of each component in the net signal also varies dramatically between aliquots, due to inter-grain differences in the strength of each component and the absorbed dose. External factors such as stimulation light intensity (and wavelength) and the level of dark noise also have a significant effect. However, for the practical purpose of maximising the fast component under 470 nm stimulation, the actual range of suitable time-intervals remains small. This is because the relative cross-sections of each component remain similar across different aliquots/grains (Jain et al., 2003), and because of the consistent removal of the slow component regardless of the exact integrals used.

The level of precision on the net OSL count also depends on time-interval choice and OSL intensity. For the samples studied here, we have found that for practical levels of precision, the percentage of the net signal coming from the fast component is maximised by keeping the background time-interval approximately 2.5 times the length of the initial interval (and immediately following it). This ratio is weakly sensitive to the intensity and dominance of the fast component; small differences in the ratio make little difference to D_e.

5.3 Implications for older samples

The removal of the slow components by using an early background is highly beneficial for young samples, because either through partial bleaching or thermal transfer the slow components are likely to cause most scatter in D_e. Furthermore, weak signal-to-noise ratios with young samples

make the extraction of the fast component through curve fitting challenging (Cunningham and Wallinga, 2009). The early background method therefore represents an extremely simple and efficient way of obtaining a predominantly fast-component derived signal.

When it comes to older samples, other sources of scatter, rather than partial bleaching, are likely to be more important. Several authors have noted a significant underestimation of age, which becomes more apparent for older samples (Murray et al., 2008; Stokes et al., 2003). Singarayer and Bailey (2003) identified a slow component 'S2' which appeared to be thermally unstable, and Rhodes et al. (2006) considered this component to be causing D_e underestimates in their bulk OSL signal. Where D_e underestimation is caused by an unstable slow component, the use of an early background is likely to be beneficial, and lead to an increase in D_e compared to the late-background approach. Recently however, Bailey (in press) suggested that an unstable medium component is present in some samples, some of which will still be included in the net signal when the early background is used. While the early-background approach is an improvement on the late-background approach for such samples, the brightness of the OSL signals for most older samples would facilitate more sophisticated methods of fast-component isolation to be used instead. This could be approached by curve-fitting of the OSL signal (although this is by no means simple, see Wallinga et al. 2008); or through IR stimulation (Bailey, in press) or IR depletion (Jain et al., 2005).

5.4 The ultrafast component

Jain et al. (2003, 2008) have detected an ultrafast OSL component in several quartz samples. The low thermal stability of the ultrafast component makes it unsuitable for dating, and its presence in regenerative signals can lead to dose underestimation. Even a small ultrafast component will have a significant effect on D_e. As the signal from the ultrafast component is completely removed after 0.15 s, it is always contained within the initial signal interval. As such, the proportion of the net signal constructed from the ultrafast component is largely unaffected by the choice of intergration time-intervals, but is negatively correlated with net signal intensity. The use of an early background therefore has no adverse effects with respect to the ultrafast component compared to a late background. To avoid influence of the ultrafast component on the D_e estimate, IR bleaching may be beneficial (Wallinga et al., 2010).

6. Conclusion

When using integration intervals of CW-OSL data for the purpose of dating, the choice of time-intervals influences the proportion of each OSL component in the net OSL count, and the error due to counting statistics. We have tried to identify which combination of time-intervals should be used for dating, when the stimulation wavelength is 470 nm, and conclude that:

1. By using a background interval which immediately follows the interval for the initial signal (rather than at the end of the stimulation period), the proportion of fast component in the net OSL count is much improved, while the proportion of slow components is diminished by approximately one order of magnitude.
2. For a specified (and practical) level of precision, the proportion of the net OSL count coming from the fast component can be maximised by using a background interval approximately 2.5 times longer than the initial signal (and immediately following it)

For two young samples of known age, we found that (with the stimulation power at 35 mW cm^{-2}) an initial signal of 0 - 0.40 s with background interval from 0.40 - 1.40 s produced results showing less thermal transfer, less recuperation, tighter D_e distributions and more aliquots with D_e in line with the expected D_e than using the alternative, late background time intervals. We consider this improvement to be largely due to the almost complete removal of the slow components from the net signal. Given that the use of an early background is extremely easy to implement and does not seem to have any detrimental effects, we suggest it should be used routinely to improve the accuracy of quartz OSL dating.

Acknowledgements

The authors are sponsored by NWO/STW grant DSF.7553. We thank Denise Maljers for sample NCL-3505030, and Jan Willem de Kort and Jan van Doesburg for sample NCL-9908154. Marcel Bakker, Tammy Rittenour, Jon Olley and Bert Roberts are thanked for their comments on an earlier version of our manuscript. We also owe thanks to Andrew Murray for encouraging us to pursue this topic.

References

Aitken, M.J., Xie, J., 1992. Optical dating using infrared diodes: young samples. Quaternary Science Reviews 11,147-152.

Bailey, R.M. in press. Direct measurement of the fast component of quartz optically-stimulated luminescence and implications for the accuracy of optical dating. Quaternary Geochronology (2009), doi: 10.1016/j.quageo.2009.10.003

Bailey, R.M., Smith, B.W., Rhodes, E.J., 1997. Partial bleaching and the decay form characteristics of quartz OSL. Radiation Measurements 27, 123-136.

Bakker, M.A.J., Maljers, D., Weerts, H.J.T., 2007. Ground-penetrating radar profiling on embanked floodplains. Netherlands Journal of Geosciences - Geologie en Mijnbouw 86, 55-61.

Ballarini, M. 2006. Optical dating of quartz from young deposits. PhD Thesis, Delft University of Technology.

Ballarini, M., Wallinga, J., Wintle, A.G., Bos, A.J.J., 2007. A modified SAR protocol for optical dating of individual grains from young quartz samples. Radiation Measurements 42, 360-369.

Banerjee, D., Bøtter-Jensen, L., Murray, A.S., 2000. Retrospective dosimetry: estimation of the dose to quartz using the single-aliquot regenerative-dose protocol. Applied Radiation and Isotopes 52, 831-844.

Bøtter-Jensen, L., Bulur, E., Duller, G.A.T., Murray, A.S. 2000. Advances in luminescence instrument systems. Radiation Measurements 32, 57-73.

Cunningham, A.C., Wallinga, J., 2009. Optically Stimulated Luminescence dating of young quartz using the fast component. Radiation Measurements 44, 423-428.

Cunningham, A.C., Wallinga, J., van Heteren, S., Bakker, M.A.J., van der Valk, L., Oost, A.P., van der Spek, A., 2009. Optically stimulated luminescence dating of storm surge sediments: a test case from the Netherlands. In Wallinga, J. and Storms, J. (eds) NCL Symposium series, Volume 6.

Doesburg, J. van, Kort, J.W. de, Schut, P.A.M., 2010. IJzer en aarde. Waarderend onderzoek naar een ringvormig aardwerk in Appel (gemeente Nijkerk) in 2008, Rapport Archaeologische Monumentenzorg, Rijksdienst voor het Cultureel Erfgoed, Amersfoort

Galbraith, R.F., Roberts, R.G., Laslett, G.M., Yoshida, H., Olley, J.M., 1999. Optical dating of single and multiple grains of quartz from jinmium rock shelter, northern Australia, part 1, Experimental design and statistical models. Archaeometry 41, 339-364.

Hobo, N., Makaske, B., Middelkoop, H., Wallinga, J. 2010. Reconstruction of floodplain sedimentation rates: a combination of methods to optimize estimates. Earth Surface Processes and Landforms DOI: 10.1002/esp.1986

Huntley, D.J., Hutton, J.T., Prescott, J.R., 1993. Optical dating using inclusions within quartz grains. Geology 21, 1087-1090.

Jain, M., Murray, A.S., Bøtter-Jensen, L., 2003. Characterisation of blue-light stimulated luminescence components in different quartz samples: implications for dose measurement. Radiation Measurements 37, 441-449.

Jain, M., Thomsen, K.J., Bøtter-Jensen, L., Murray, A.S., 2004. Thermal transfer and apparent-dose distributions in poorly bleached mortar samples: results from single grains and small aliquots of quartz. Radiation Measurements 38, 101-109.

Jain, C., Murray, A.S., Bøtter-Jensen, L., Wintle, A.G., 2005. A single-aliquot regenerative-dose method based on IR (1.49 eV) bleaching of the fast OSL component in quartz. Radiation Measurements 39, 309-318.

Jain, M., Choi, J.H., Thomas, P.J., 2008. The ultrafast OSL component in quartz: Origins and implications. Radiation Measurements 43, 709-714.

Li, B., 2007. A note on estimating the error when subtracting background counts from weak OSL signals. Ancient TL 25, 9-14.

Middelkoop, H., 1997. Embanked floodplains in the Netherlands. Geomorphological evolution over various timescales. PhD-thesis Utrecht University, the Netherlands.

Murray, A.S., Wintle, A.G., 2000. Luminescence dating of quartz using an improved single-aliquot regenerative-dose protocol. Radiation Measurements 32, 57-73.

Murray, A.S., Wintle, A.G., 2003. The single aliquot regenerative dose protocol: potential for improvements in reliability. Radiation Measurements 37, 377-381.

Murray, A., Buylaert, J.P., Henriksen, M., Svendsen, J.I., Mangerud, J., 2008. Testing the reliability of Quartz OSL ages beyond the Eemian. Radiation Measurements 43, 776-780.

Rhodes, E.J., Singarayer, J.S., Raynal, J.P., Westaway, K.E., Sbihi-Alaoui, F.Z., 2006. New age estimates for the Palaeolithic assemblages and Pleistocene succession of Casablanca, Morocco. Quaternary Science Reviews 25, 2569-2585.

Singarayer, J.S., Bailey, R.M., 2003. Further investigations of the quartz optically stimulated luminescence components using linear modulation. Radiation Measurements 37, 451-458.

Singarayer, J.S., Bailey. R.M., 2004. Component-resolved bleaching spectra of quartz optically stimulated luminescence: preliminary results and implications for dating. Radiation Measurements 38, 111-118.

Smith, B.W., Rhodes, E.J., 1994. Charge movements in quartz and their relevance to optical dating. Radiation Measurements 23, 329-333.

Singhvi, A.K., Lang, A., 1998. Improvements in infra-red dating of partially bleached sediments – the 'Differential' Partial Bleach Technique. Ancient TL 16, 63-71.

Stokes, S., Ingram, S., Aitken, M.J., Sirocko, F., Anderson, R., Leuschner, D., 2003. Alternative chronologies for Late Quaternary (Last Interglacial-Holocene) deep sea sediments via optical dating of silt-sized quartz. Quaternary Science Reviews 22, 925-941.

Truelsen, J.L., Wallinga, J., 2003. Zeroing of the OSL signal as a function of grain size: investigating bleaching and thermal transfer for a young fluvial sample. Geochronometria 22, 1-8.

Tsukamoto, S., Rink, W.J., Watanuki, T., 2003. OSL of tephric loess and volcanic quartz in Japan and an alternative procedure for estimating D_e from a fast OSL component. Radiation Measurements 37, 459-465.

Wallinga, J., Murray, A.S., Bøtter-Jensen, L., 2002. Measurement of the dose in quartz in the presence of feldspar contamination. Radiation Protection Dosimetry 101, 367-370.

Wallinga, J., Bos, A.J.J., Duller, G.A.T., 2008. On the separation of quartz OSL signal components using different stimulation modes. Radiation Measurements 43,742-747.

Wallinga. J., Hobo, N., Cunningham, A.C., Versendaal, A.J., Makaske, B., Middelkoop, H., 2010. Sedimentation rates on embanked floodplains determined through quartz optical dating. Quaternary Geochronology 5, 170-175.

Wintle, A.G., Murray, A.S., 2006. A review of quartz optically stimulated luminescence characteristics and their relevance in single-aliquot regeneration dating protocols. Radiation Measurements 41, 369-391

Figure and Table Captions

Fig. 1. The influence of OSL integration time-intervals on the composition of the net signal for a simulated decay curve. Gridded surfaces show the percentage of (a) fast component, (b) medium component and (c) slow component, and also (d) the relative error (RSE) on the net count. In all cases the background interval immediately follows the initial signal interval. The grey shaded horizontal planes in (a), (b) and (c) indicate the values derived from using the late background combination of time-intervals (0 - 0.30s for initial signal; 36 - 40s for background). In (d) the shaded plane indicates an RSE of 5%. The black square indicates the combination of time intervals that (in this example) maximise the fast-component proportion of the net signal while keeping the RSE below 5%. Please note the different scales used for the 'signal length' axis and the 'BG length' axis.

Fig. 2. A check on the suitability of a three-component model of OSL decay for the samples studied here. The (CW)-OSL was measured following a regenerative dose, and is plotted on a log-log scale to improve visibility.

Fig. 3. The integration time-intervals which result in the net signal with the largest proportion of fast component, for a given RSE threshold. (a) and (b) show calculations for different aliquots of sample NCL-3505030. The proportion of the net signal composed of fast component, resulting from the specified combination of time-intervals, is shown on the right-hand axis. Insets show the OSL decay curves for these aliquots, which were fitted with three exponential functions so that the effects of time-interval selection could be ascertained.

Fig. 4. The calculated ratio of background length to initial-signal length which gives the net signal with the maximum possible proportion of fast component, for RSE thresholds between 1 and 15 % on the (first) regenerative OSL signal. Each line represents one aliquot, the decay curve of which has been fitted with three exponential functions to represent the fast, medium and slow components so that the effects of using different integration intervals can be calculated. Within each sub-plot, the lines are shaded according to the estimated strength of the fast component (n_{01}) for that aliquot, with darker shading for larger fast components. The shading scale differs between samples. The dashed line indicates a ratio of 2.5. Also shown is the average percentage of fast component in the net signal (open symbols, plotted on the second y-axis), when calculated using

the optimum integration lengths (this means that the integration lengths vary between aliquots at any one threshold). OSL measurements used in plot (d) were carried out on a reader with a higher stimulation power.

Fig. 5. (a-b) Example OSL decay curves for two samples, showing the natural and regenerative signals. Also shown are the integration intervals suggested in this paper to be suitable for these samples. (c-d) The thermally transferred dose (given as a percentage of the expected dose) as a function of preheat temperature, details in Section 4.3. (e-f) Results of dose recovery tests following a given dose of ~3.2 Gy, under the same conditions used for measurement of D_e.

Fig. 6 (a) Probability density functions (PDFs) of D_e calculated using both early background (0-0.40 s; 0.40-1.40 s) and late background (0-0.30 s; 36-40 s) intervals, for sample NCL-3505030. (b) and (c) show the same data in radial plot form. The shaded regions indicate values within 2 s.e. of the mean expected age. Similarly, (d) shows the PDFs for sample NCL-1109004, with the radial plots in (e) and (f).

Fig.7. Examples in the use of an early background, using samples of different OSL sensitivity. On the left, sample NCL-1107136 (very young fluvial sample); on the right, sample NCL-9908154. (a) and (b) show typical OSL decay curves, with the early background intervals indicated (see section 4.2). Please note that the channel step-size differs between these samples (0.02 s and 0.025 s, both shorter than in the previous examples (Fig. 5)). In addition, OSL measurements for plot (b) were carried out under higher stimulation power, leading to faster OSL decay. (c) and (d) show probability density functions of the D_e distributions calculated using the indicated early background intervals (shaded area) and the standard late-background intevals (solid line).The PDFs have been normalised by area. Numbers in brackets indicate [Number of accepted aliquots / Total Number of aliquots measured].

Table 1. Details of the SAR protocol used for each sample.

Table 2. Standard tests for each sample, calculated with both early and late backgrounds. Age control for the latter two samples is speculative or absent, so direct comparisons have not been made.

Figure 1 colour

Click here to download high resolution image

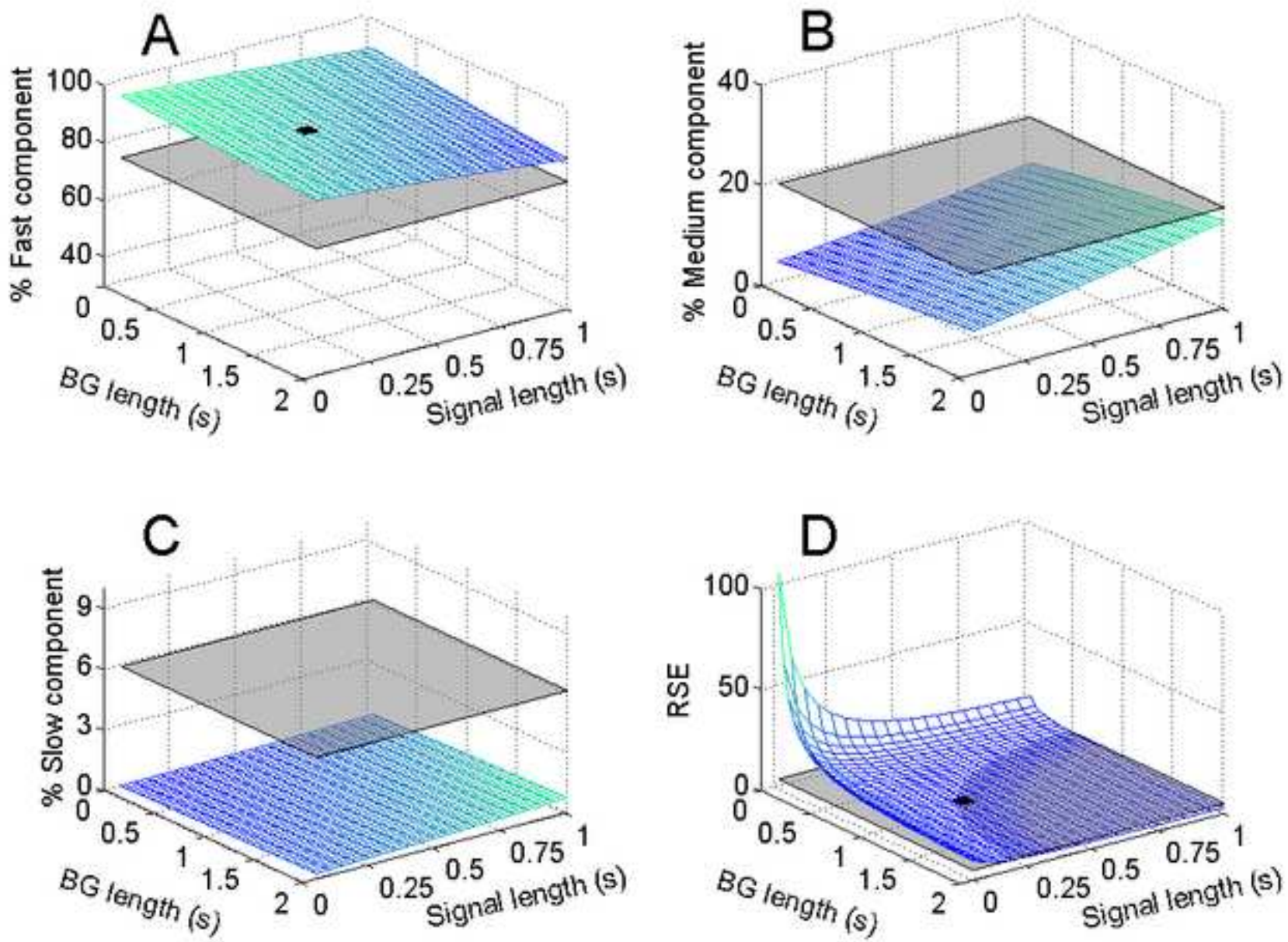

Figure 1 BW

Click here to download high resolution image

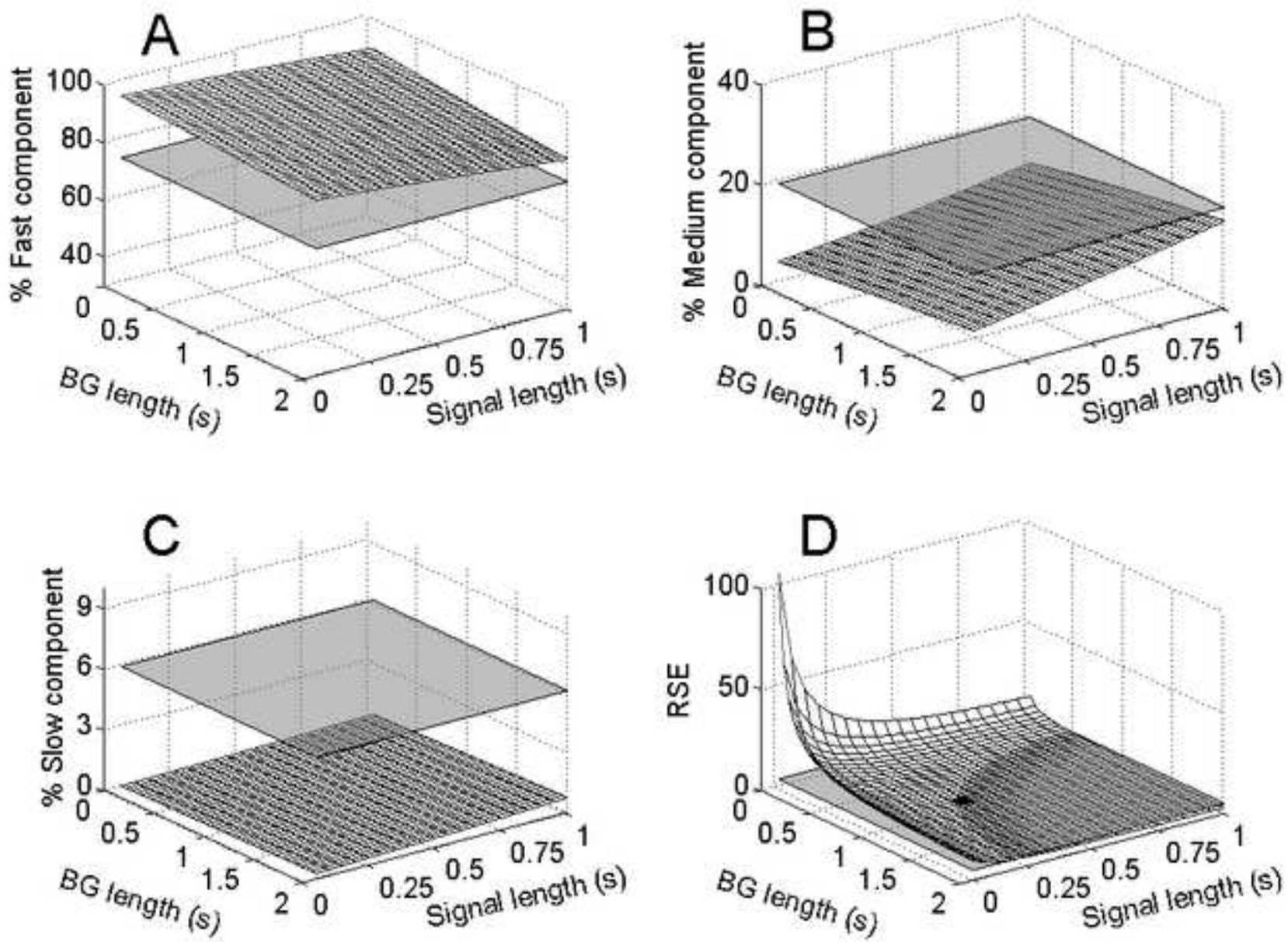

Figure 2

Click here to download high resolution image

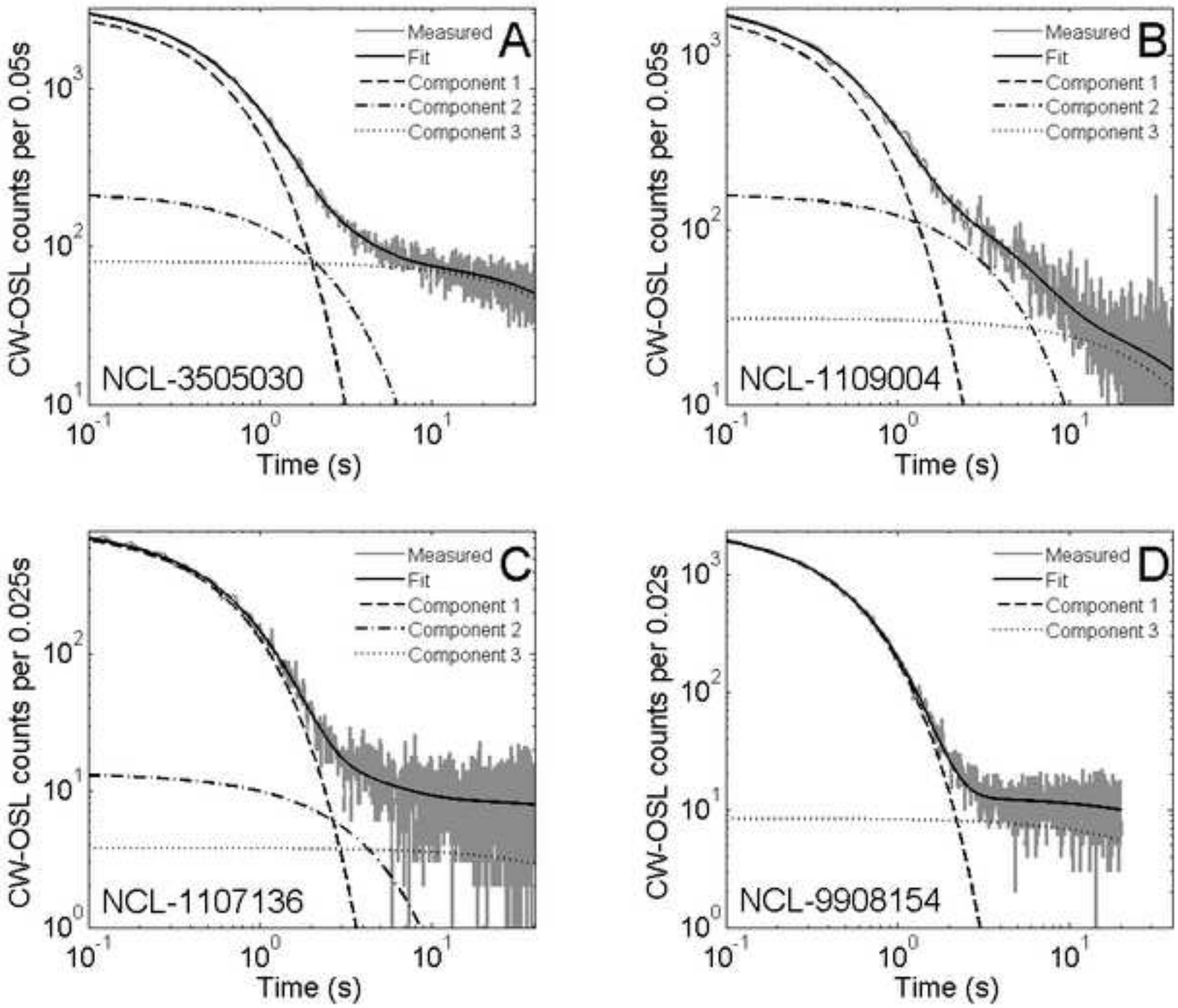

Figure 3 colour

Click here to download high resolution image

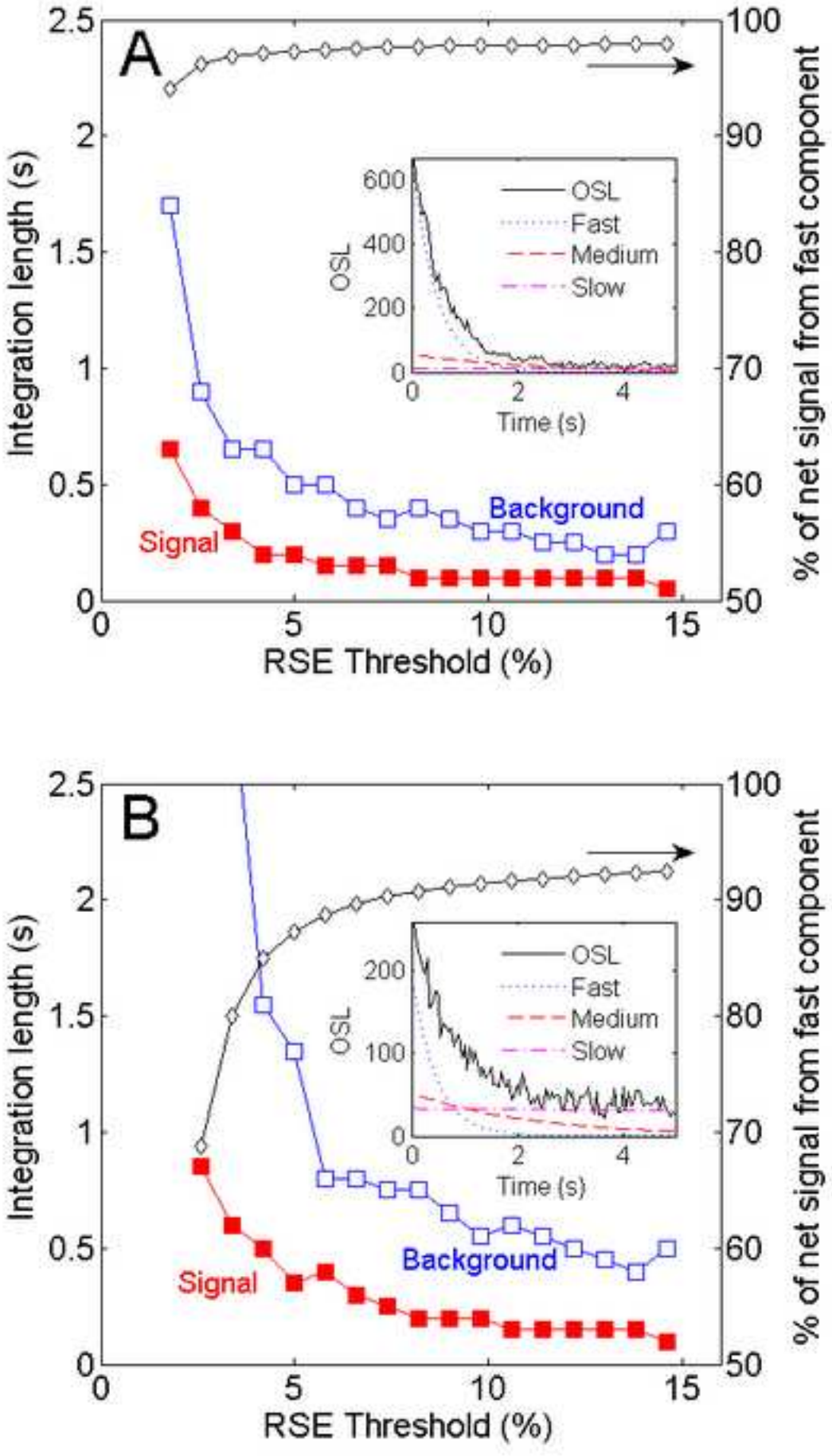

Figure 3 BW

Click here to download high resolution image

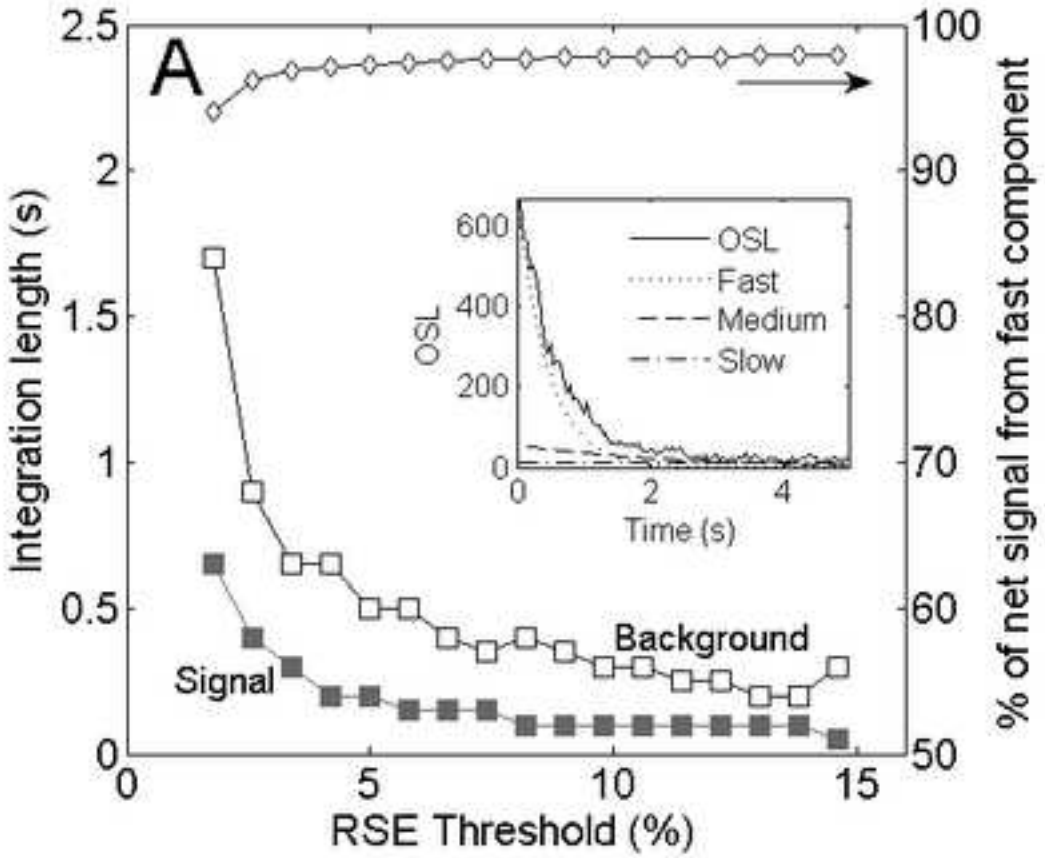

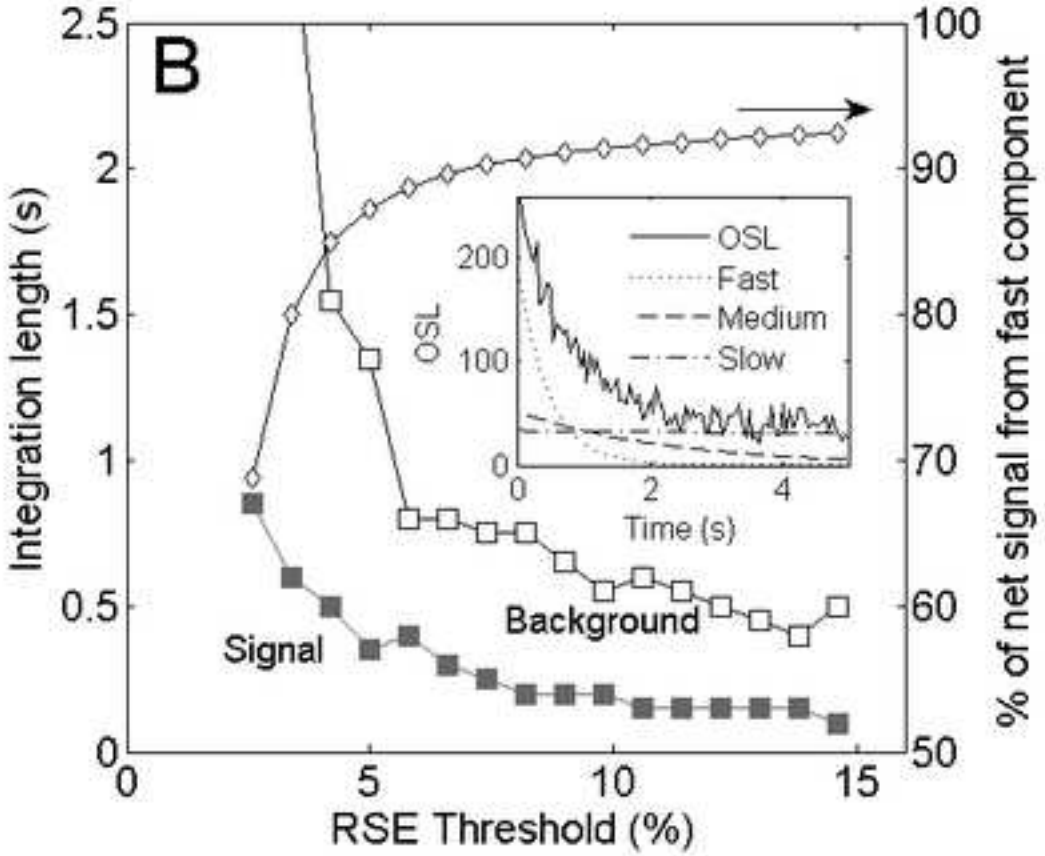

Figure 4

Click here to download high resolution image

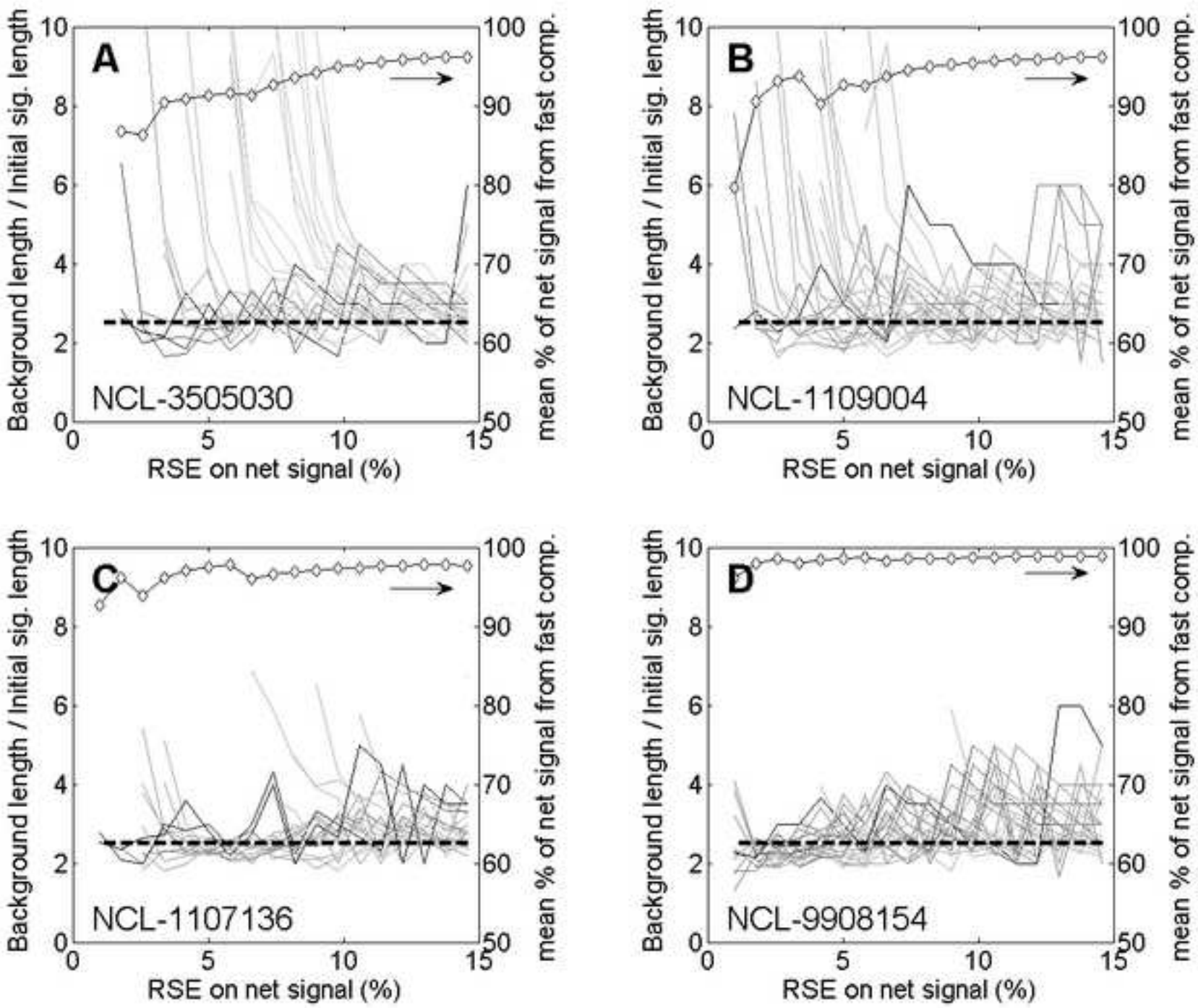

Figure 5

Click here to download high resolution image

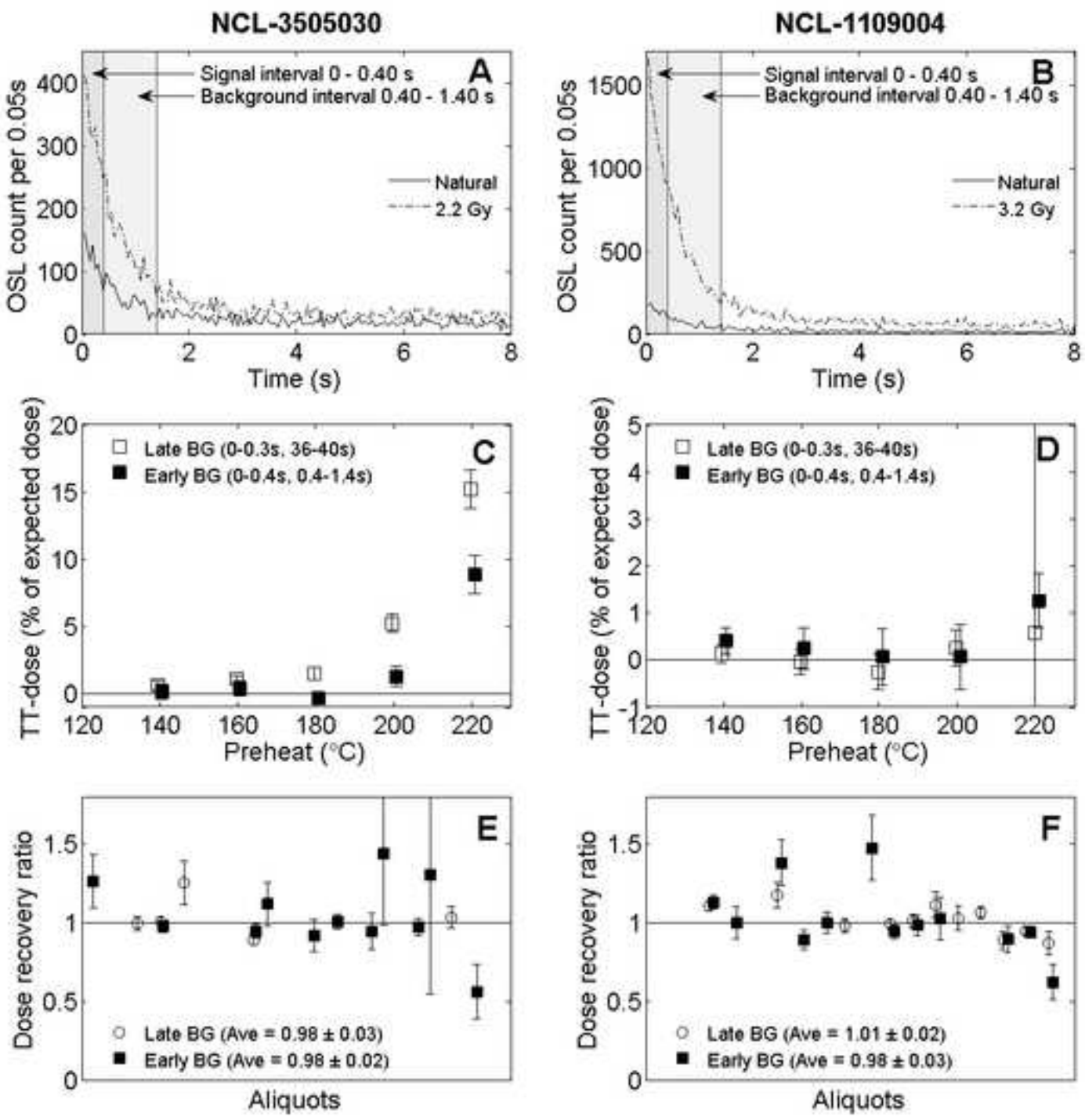

Figure 6

Click here to download high resolution image

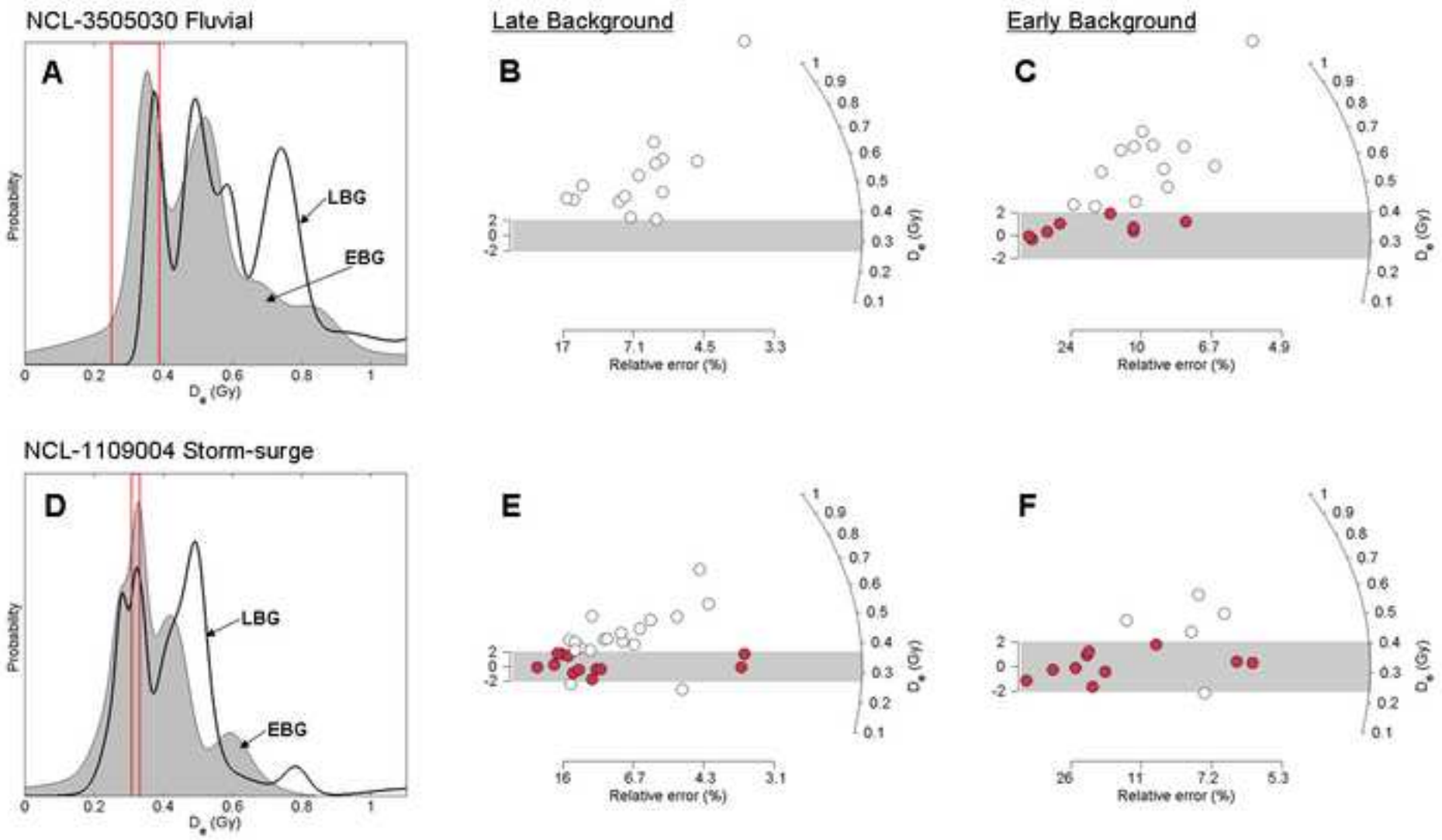

Figure 7

Click here to download high resolution image

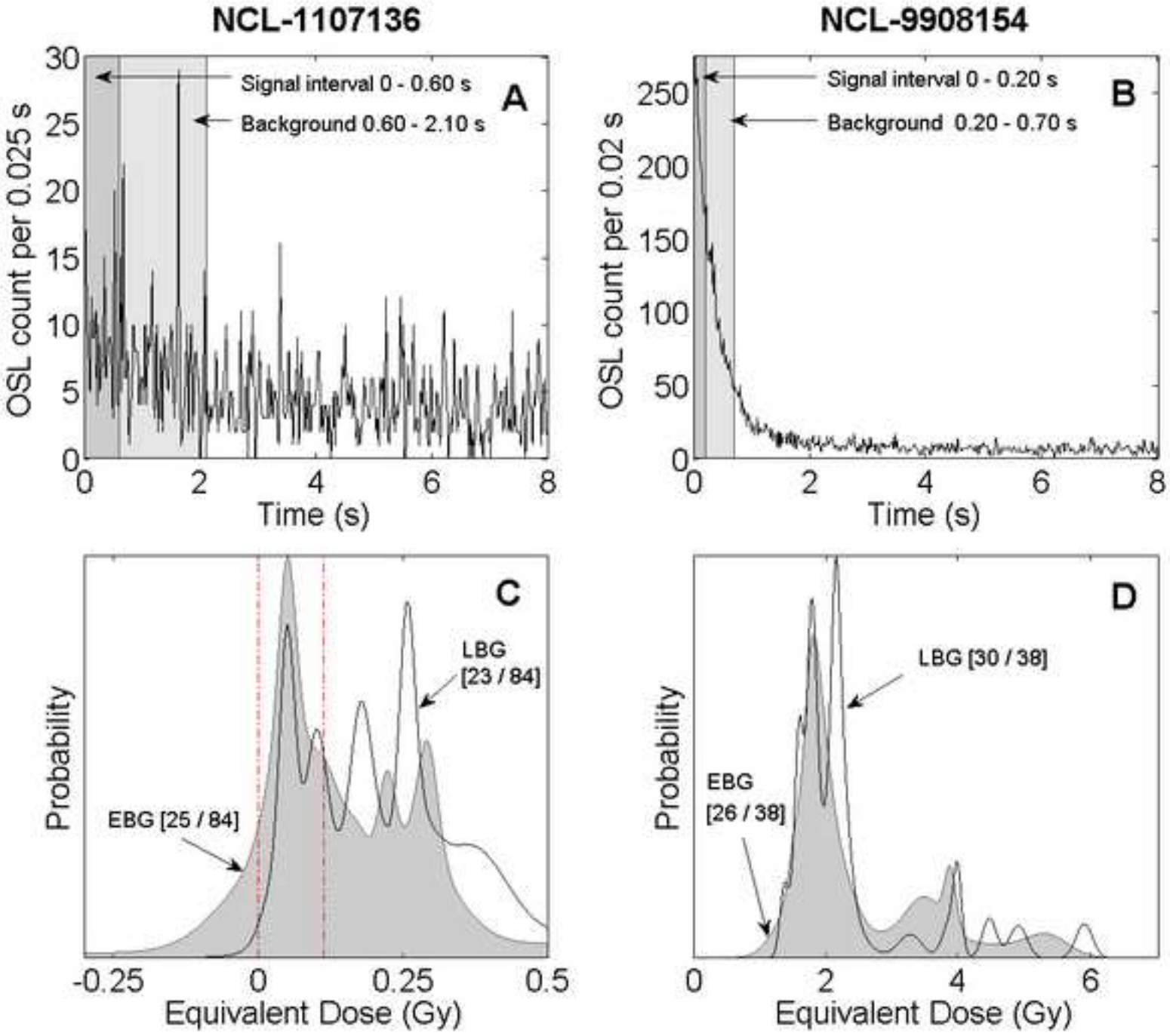

Table 1

Step	Treatment	NCL-3505030	NCL-1109004	NCL-1107136	NCL-9908154
1	Dose	N, 2.2, 0, 2.2 Gy	N, 3.2, 0, 3.2 Gy	N, 5, 0, 5 Gy	N, 5, 10, 15, 0, 5 Gy
2	Preheat	200ºC for 10s	180ºC for 10s	200ºC for 30s	240ºC for 10s
3	IR Bleach (875 nm)	175ºC for 40s	-	a	-
4	OSL (470 nm)	125ºC for 40s	125ºC for 40s	125ºC for 40s	125ºC for 20s
5	Test dose	2.2 Gy	3.2 Gy	5 Gy	5 Gy
6	Cutheat	200ºC	170ºC	200ºC	220ºC
7	IR Bleach (875 nm)	175ºC for 40s	-	a	-
8	OSL (470 nm)	125ºC for 40s	125ºC for 40s	125ºC for 40s	125ºC for 20s
9	OSL Bleach (470 nm)	220ºC for 40s	180ºC for 40s	220ºC for 40s	250ºC for 40s

[a]This protocol used a 20s IR bleach during the preheat and cutheat steps (see Wallinga et al., 2010)

Table 2

Sample	Time-intervals	Recycling ratio	Recup. dose (Gy)	No. Accepted / Total aliquots	No. giving expected D_e [a]
NCL-3505030	Late BG	0.996 ± 0.016	0.033 ± 0.006	14 / 48	2
	Early BG	0.980 ± 0.020	0.011 ± 0.005	21 / 48	7
NCL-1109004	Late BG	0.997 ± 0.010	0.007 ± 0.003	30 / 48	12
	Early BG	0.988 ± 0.015	-0.008 0.006	15 / 48	11
NCL-1107136	Late BG	0.972 ± 0.009	0.034 ± 0.006	23 / 84	-
	Early BG	0.970 ± 0.009	0.026 ± 0.004	25 / 84	-
NCL-9908154	Late BG	1.022 ± 0.009	0.011 ± 0.002	30 / 38	-
	Early BG	1.020 ± 0.014	0.007 ± 0.003	26 / 38	-

[a] Agreement within 2σ. Uncertainty in the dose rate has been included, hence the small difference with Fig. 5.